International Journal of Innovative Computing, Information and Control
Volume **15**, Number **1**, February **2019**

ICIC International ©2019 ISSN 1349-4198
pp. **107–127**

THE RELATIONSHIP BETWEEN THE CLIMATIC INDICES AND THE RAINFALL FLUCTUATION IN THE LOWER CENTRAL PLAIN OF THAILAND

Korrakoch Taweesin* and Uma Seeboonruang

Department of Civil Engineering
Faculty of Engineering
King Mongkut's Institute of Technology Ladkrabang
Chalongkrung Rd., Ladkrabang, Bangkok 10520, Thailand
*Corresponding author: kola592@hotmail.com

Received April 2018; revised August 2018

Abstract. *Global climate changes are revealing the interconnections between natural conditions, natural resources, and regional climate variability that may affect the rain fluctuation. Rainfall plays an important role in the process of hydrology. This research presents an analysis of rainfall in the lower central plain of Thailand and the climate variability/oceanographic events in the wider geographical region, including the El Niño/Southern Oscillation (ENSO), Asian Summer Monsoon (ASM), and Indian Ocean Dipole (IOD). Data from 1980-2010 and 2011-2014 were collected for calibration and verification. Next, the frequency domains, spectra, and wavelet transforms were analyzed, together with the climate index and rainfall. The results revealed that rainfall occurs in seasons, yearly cycles, and off-seasons. The behavior of ASMs, for example, Indian Summer Monsoon Index (IMI) and Western North Pacific Monsoon Index (WNPMI), is the most similar to that of rainfall events, while the similarity of the other indices to rainfall events is not so strong. Cross-correlation analysis showed that there were delays between the climate indices and rainfall, so that multiple linear regression with lag time is required for further analysis. The results illustrate that the cross-correlation coefficients of IMI and WNPMI with rainfall are both approximately 0.6. The multiple regression with lag time shows that the average multiple coefficient correlation (R) is 0.64. The indicator of the summer monsoon index value is WNPMI, which is the most influential factor for rainfall. Finally, the proposed equations, based on the cross-correlation and multiple-linear regression with lag time techniques, can be used to predict precipitation and be applied to the development of rainfall forecasting in the future.*

Keywords: Climate indices, Multiple-linear regression, Cross-correlation, Climate variability

1. **Introduction.** It is widely accepted that the world's weather is changing [1], which can be seen from the variability of the weather and changes in the climate in many parts of the world [2]. Every aspect of the environment is involved in this climate variability – particularly the atmosphere, ocean levels, and average temperature – resulting in changes in season timing and rain distribution [3]. Studies from the Intergovernmental Panel on Climate Change (IPCC) in 2013 [4] showed that the average world temperature from 1906-2005 had increased by 0.6-0.9 degrees Celsius. This resulted in increased melting of the polar ice and the expansion of the ocean area; the average sea level rose at an average rate of 1.8 mm per year over 1961-2003 and there was greater variability in the distribution of rain, which could result in more severe drought and flooding.

DOI: 10.24507/ijicic.15.01.107

Thailand, which is located in the Southeast Asia region, is affected by climate variability caused by the interaction between the ocean, atmosphere, and the ground in the equatorial area between the Indian Ocean and the Pacific Ocean. Two important climate variability phenomena in this area are the Indian Ocean Dipole (IOD) and the El Niño-Southern Oscillation (ENSO). In addition, the climate variability behavior was analyzed in time domain such as the study of severity and cycles of IOD [5] and the finding of the similar return period between IOD and ENSO [6]. Moreover, the signal transformation principle from the time domain to the frequency domain was applied to the climate data, such as the spectral analysis and the wavelet analysis, to better considering the return period of the climate variability phenomenon [7,8]. These studies of climate variability to understand the effect on water resources and the preparation of water management are essential.

In the field of hydrology, the forecast of rainfall is important since water resource allocation could be more effective if the rainfall forecasts were more accurate, and because rainfall plays an important role in several fields of hydrology. Today, it is common to study rainfall forecasts. Terzi and Çevik [9] studied the rainfall forecasts in Isparta, Turkey, by means of multiple regression. In Thailand, Tingsanchali and Gautam [10] studied the forecasts of rainfall change all over the country, and Singhrattna et al. [11] studied rain forecasts from the summer monsoon by using linear regression and nonparametric regression.

The objectives of this study are to investigate the climate/oceanography indices' patterns using regression analysis to predict monthly rainfall in the lower central plain of Thailand and the vicinity of Bangkok. The index data studied comprised the seawater surface-temperature anomaly index in the Indian Ocean (DMI), the Southern Oscillation Index (SOI), the Multivariate ENSO Indicator (MEI), the seawater temperature in the Pacific Ocean (NINO4), as well as the Indian Monsoon Index (IMI), and the Western North Pacific Monsoon Index (WNPMI). The areas studied are zones of high population density, major industry, and agriculture.

2. **Literature Review.** Two kinds of monsoons have an impact on Thailand: the Southwest Monsoon – also known as the Asian Summer Monsoon (ASM) – occurring May-October, and the North-Eastern Monsoon which occurs in October-December. The Asian Summer Monsoon, blanketing the Bay of Bengal, originated at the Indonesia Peninsula, affects South Asia and Southeast Asia by carrying humid air from the Indian Ocean and generating rainfall in Thailand [12].

According to data from Thailand's Meteorological Department, recorded from 1951-2002, rainfall in Thailand has been reducing; meanwhile, the minimum and maximum temperatures are tending to decrease and to increase, respectively. Water resources around the world appear to be responsive to the variability of climate from the past few years to decades [2,13]. The regional climate condition consists of several kinds of climate variability; the most well-known is the El Niño-Southern Oscillation (ENSO) phenomena, which has a time period of between 2 and 6 years [14].

Mantua and Hare [15] and Minobe [16] presented information on variability in the Pacific Decadal Oscillation (PDO), occurring approximately every 10-25 years and 50-70 years. The PDO is the large natural phenomenon caused by the change of sea water surface temperature between the east and the west sides of the Pacific Ocean, so it is similar to the ENSO but has a longer periodicity. In addition, the variability of the North Atlantic Oscillation (NAO), with a period of 7-8 years, was described by Fye et al. [17]. The importance of the Atlantic Multidecadal Oscillation (AMO), with a return period at around 50-80 years, was revealed by Kerr [18].

Factors in climate variability include temperature, moisture, wind, and rain fluctuations, which are the most important elements of the hydrological cycle. McBride and Nicholls [3] and Chiew et al. [19] investigated the relationship between rainfall and climate variability in Queensland, Australia. Hanson et al. [2] found similar relationships to those in Queensland in the American Southwest. Furthermore, Mantua and Hare [15] and Wolter and Timlin [20] found that the patterns of ENSO and PDO are similar when the weather is warmer and more humid. On the other hand, the patterns of ENSO and PDO are opposite to each other when the weather is cold and dry. Cayan [21] found that rainfall and river water in the American Southwest are affected by a connection to the ENSO index in cycles of 2-6 years.

Thailand is impacted by climate differences originating from the Indian Ocean and the west coast of the Pacific Ocean. Limsakul et al. [22] found that the accumulated annual rainfall decreases in the years El Niño occurs and increases in the years La Niña occurs. Kusreesakul [23] and Limsakul and Goes [24] found a link between the climate index and changes in rainfall both in time periods of less than a decade and in multidecadal periods. It can be argued, therefore, that ASM, IOD, and ENSO are influential in climate oscillation in this region. Furthermore, Limsakul et al. [25] found that the annual period of rainfall is related to the summer monsoon originating in South Asia (IMI), and the summer monsoon originating in the northwestern part of the Pacific Ocean (WNPMI). From the information from these studies, it is concluded that rainfall and climate variability in Thailand relates to certain periods of time; for example, cycles of seasons, within decades, or over multidecadal time periods.

3. **Methodology.**

Based on the results of previous research, such as that by Singhrattna et al. [11,25], this study makes the assumption that there will be a connection between climate oscillation and rainfall in the study area. Therefore, rainfall data and climate condition indices were collected and analyzed in order to explain how these factors influence rainfall change and forecasting. The study area covered about 16 provinces of Thailand's lower central plain.

The study is divided into three major parts: (1) studying the return period in frequency, in terms of rainfall and the selected climate indices; (2) finding the relationship between the rain and climate indices using cross-correlation, in order to develop the regression equation; and (3) comparing the rainfall calculated from the regression equation with the observed data.

3.1. **Data.**

3.1.1. *Rainfall.* Statistical data of the average monthly rainfall in the lower central plain of Thailand were collected from the Meteorological Department. Fifteen stations in the lower central region were studied, including Bangkok station, Don Muang station, Chachoengsao station, Samut Prakarn station, Suvarnabhumi station, and Nakhon Pathom station, among others. The primary statistics included mean, median, and standard deviation. The length of time covered by the rainfall data is varied, so the length of the data interval was selected in accordance with the climate condition index. In addition, the length of time spanned by the data should not be less than 20 years in order to be able to use this data to explain the characteristics of rainfall variability in the following years and decadal. In the study, rainfall data derived from 1980-2015 were selected. According to the primary data analysis, the highest amount of rainfall during the study period was 676.3 mm/month at the Bangkok station. The descriptive statistics of some examples of the monthly rainfall data are shown in Table 1.

TABLE 1. Descriptive statistics of monthly rainfall in the studied areas

Station	Mean (mm)	SD (mm)	Variance (mm^2)	Kurtosis	Skewness	Max (mm)
Chainat	86.49	94.46	8,902.00	1.89	1.36	462.3
Suphan Buri	81.93	90.16	8,111.08	2.62	1.48	502.2
Ayutthaya	90.34	94.87	8,957.98	0.85	1.13	463.4
Pathum Thani	117.45	109.54	11,930.67	1.58	1.14	535.6
Nakhon Pathom	85.00	94.07	8,826.21	1.88	1.39	479.0
Bangkok	130.34	131.72	17,351.84	−0.09	0.85	676.3
Nakhon Sawan	96.63	96.18	9,206.94	0.98	0.98	588.0

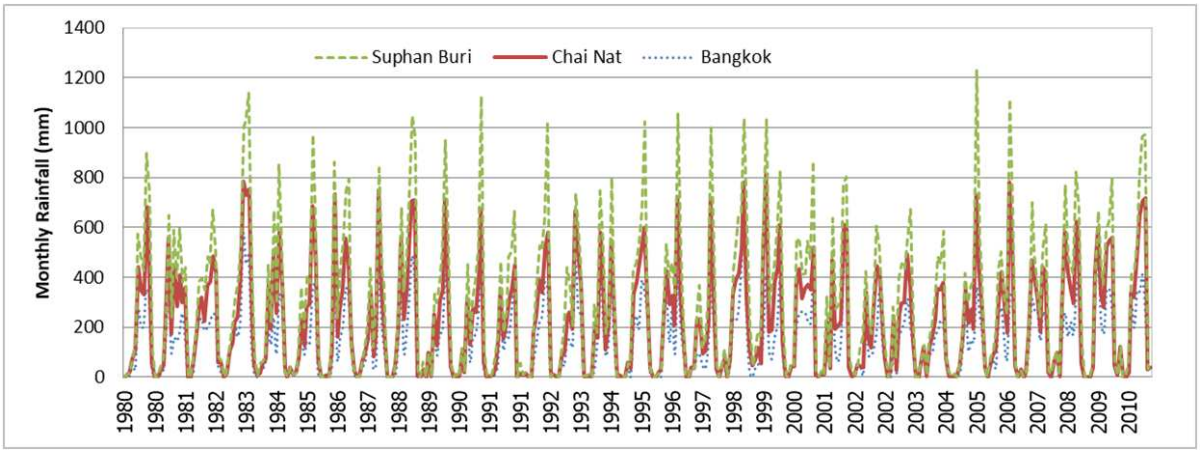

FIGURE 1. The characteristics of monthly rainfall and the examples derived from various stations

3.1.2. *Climate indices.* According to the National Oceanic and Atmospheric Administration, the important climate oscillations in the study region include the Asian Summer Monsoon (ASM), Indian Ocean Dipole (IOD), and El Niño-Southern Oscillation (ENSO). The indices of the Asian Summer Monsoon were applied, which include the Indian Summer Monsoon Index (IMI) and the Western North Pacific Monsoon Index (WNPMI). Regarding IOD, the Dipole Mode Index (DMI) was used as an indicator of different values of sea surface temperature irregularity along the equator, between the west coast of the Indian Ocean (50°-70° E and 10° S-10° N) and the east coast of the Indian Ocean (90°-110° E and 10° S-0° N). There are many indicators used to measure the irregularity of ENSO; for example, the Multivariate ENSO Index (MEI), the Southern Oscillation Index (SOI), and Sea Surface Temperature (SST) measures such as NINO 1 + 2, NINO3, and NINO4. This research focused on NINO4, which is the area of the Pacific Ocean west of the equator zone located between 5° N-5° S latitude and 150° W-160° E longitude. This area had the highest sea surface temperature, as illustrated in Figure 2.

The NINO4 has an influence on many countries located in the western part of the Pacific Ocean. The six above-mentioned indices were included in the monthly data from 1960 to the present. The characteristics of the three sample indices are shown in Figure 3.

3.2. **Study area.** The lower central plain of Thailand covers an area about 150 km wide and 200 km long, starting from the Nakhon Sawan province to the Chao Phraya River estuary around the Gulf of Thailand. The entire area is a floodplain primarily composed

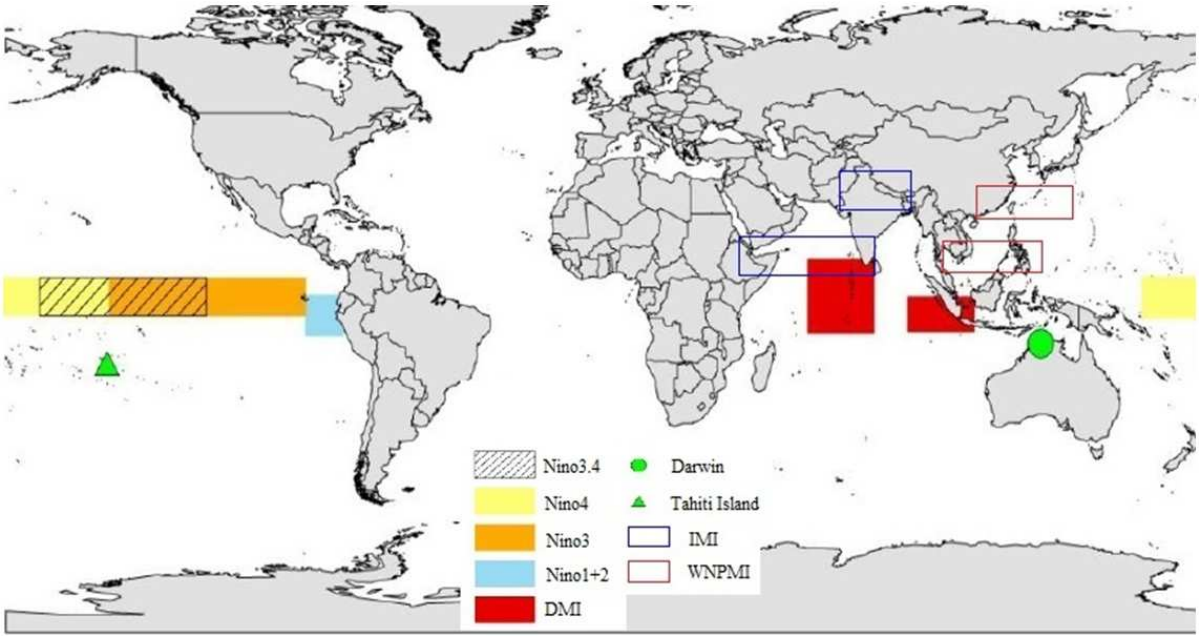

FIGURE 2. The areas of climate condition/oceanography index used in the study [26]

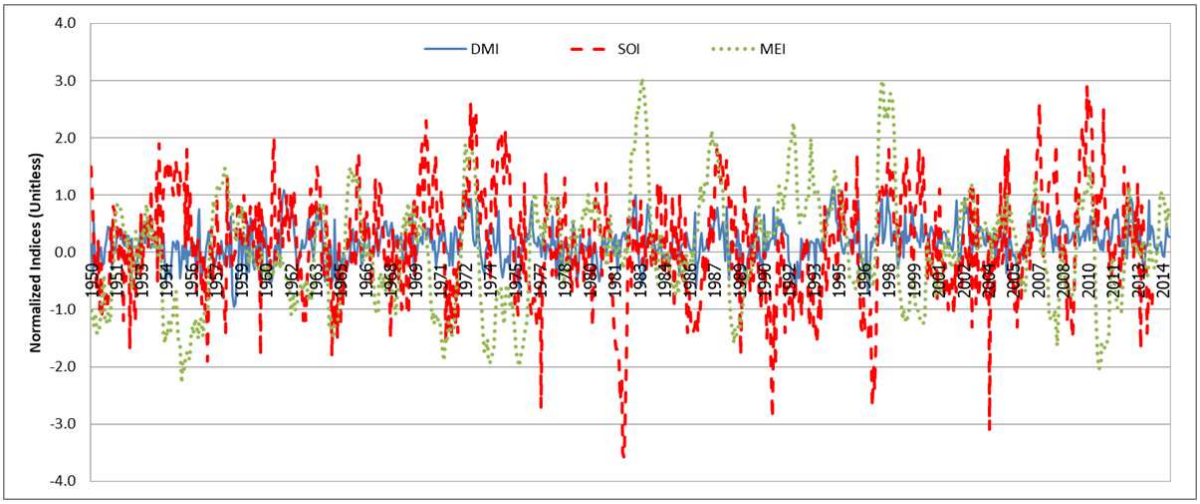

FIGURE 3. The characteristics of the sample indices: DMI, MEI, and SOI

of sediment from the Chao Phraya River, as well as its tributaries to the west of the Thacheen River and the east of the Bang Pakong River. The study area is shown in Figure 4.

3.3. **Method.** The first step was to analyze the return period of the studied variables which are (1) the summer monsoon, IOD and ENSO, which are in turn composed of six indices and (2) the rainfall, by using spectral analysis and the wavelet transform together. Spectral analysis is a fast and easy way to exhibit the periodicity of stationary data while the wavelet transform can show the periodicity over different desired durations. This step leads us to consider the recurrence period characteristics of the climate indices and the rainfall.

Spectral analysis is a method for analyzing complex data to elucidate clearer information. It can easily translate the analyzed result and is effective when the data are

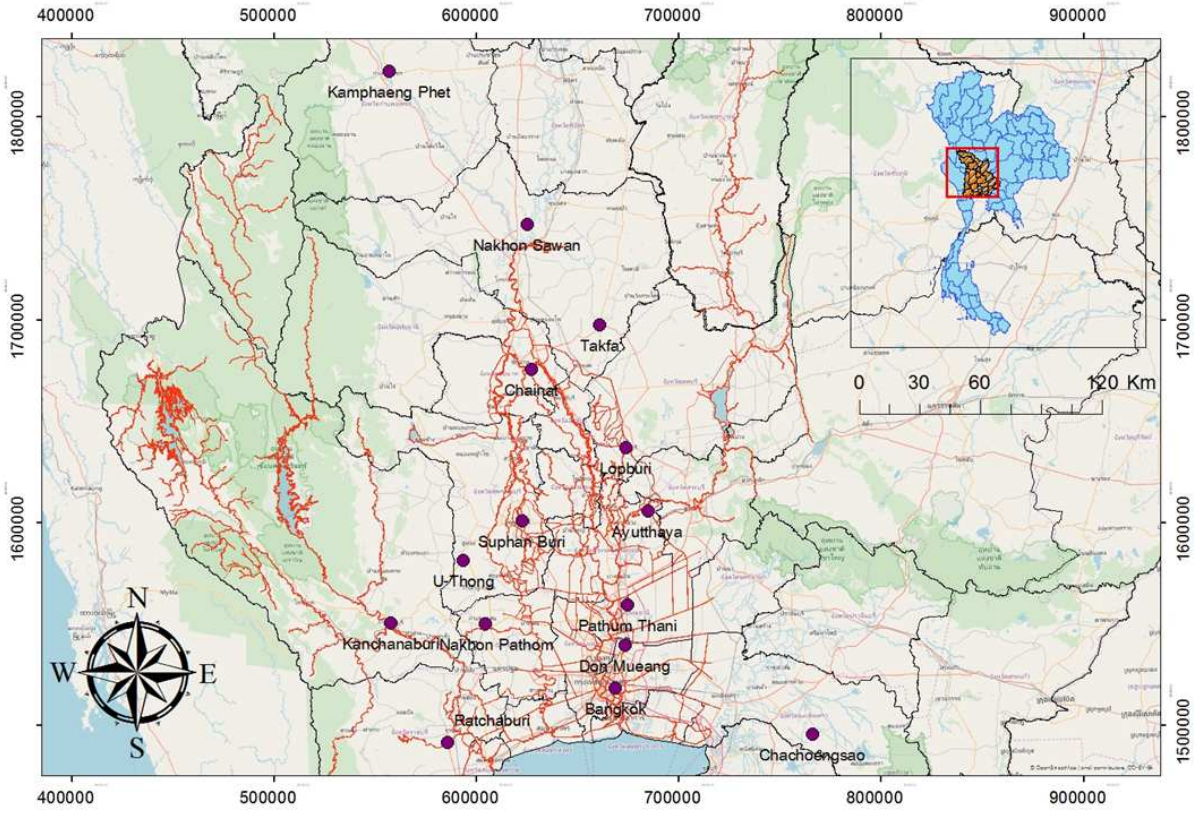

FIGURE 4. Location of the study area and rainfall gauging stations in the lower central plains of Thailand

stationary. Gu et al. [7] and Buckley et al. [8] have previously used this method for climate research.

The Fourier transform of the signal in the time domain, $x(t)$, is as follows [27]:

$$X(f) = \int_{-\infty}^{\infty} x(t) e^{-2i\pi ft} dt \tag{1}$$

$X(f)$ represents the magnitude of the component with frequency f. It can be seen that the signal is transformed completely from the time domain to the frequency domain. The time domain signal $x(t)$ can be written as an equation of the Sine and Cosine functions according to this equation:

$$x(t) = \sum_{k=1}^{q} [\beta_{k1} \cos(2\pi\omega_k t) + \beta_{k2} \sin(2\pi\omega_k t)] \tag{2}$$

where β_{k1}, β_{k2}, for $k = 1, 2, \ldots, q$, are independent zero-mean random variables with variances σ_k^2, and ω_k represents the distinct frequencies. Equation (2) exhibits the process as a sum of independent components, with variance σ_k^2 for frequency ω_k. The superposition of these spectra would result in repeated peaks in the spectrum at a frequency interval of 1/T (total duration). The return period could be considered from the spectral density estimation (the Blackman-Tukey method [28]) which smooths the spectrum in order to reduce variance. For this part of the analysis, the PAleontological STatistics (PAST) [29-31] program was used.

The climatic and rainfall data are first analyzed through spectral analysis to show the simple cyclic pattern. The wavelet transform is then applied to considering the time series data of the studied variables. This method is popular for non-stationary time series data

and was developed from the Short Time Fourier Transform (STFT) [32]. This method can also illustrate profound characteristics when the data size, the recurrence period, and the behavior change. A review of the wavelet methods was done in Seeboonruang [33] and Gurdak et al. [34].

The Continuous Wavelet Transform (CWT) of a discrete time series x_n of N observations with a time increment of δt and complex conjugate ψ^* of an analysis function $\psi(t)$ is given by:

$$W_n = \sum_{n'=0}^{N-1} x_{n'} \sqrt{\frac{\delta_t}{s}} \psi^* \left[\frac{(n'-n)\delta t}{s} \right] \tag{3}$$

where t is time, s is the wavelet scale, and n is the time variation. The analysis function $\psi(t)$ is called a mother wavelet function, which must be admissible and localized in time and frequency space, and assumes that $\psi(t)$ is normalized: $\int_{-\infty}^{\infty} \psi\psi^* d\eta = 1$. The wavelet function can adjust the window size or scale according to the data frequency. Famous wavelet functions include the Morlet, Mexican Hat, and Daubechies [35,36]. The Morlet mother wavelet was selected as the analysis function for this study because it has a reasonable number of oscillations, which ensures a good frequency resolution [37]. The Matrix Laboratory (MATLAB) program by MathWorks [38] was used for this analysis.

Next, the recurrence periods of the climate indices and the rainfall analysis results were retrieved to show whether or not the climate indices are related to the rainfall. If they are related, the cross-correlation analysis is performed on both sets of data. The results from this analysis will give the correlation coefficient (r) and the lag time between both data sets [39,40].

$$r_m = \frac{\sum (x_i - \bar{x})(y_{i-m} - \bar{y})}{\sqrt{\sum (x_i - \bar{x})^2 \sum (y_{i-m} - \bar{y})^2}} \tag{4}$$

where r_m is the correlation coefficient at the m lag time. The calculated correlation coefficient is the number that identifies how much and how closely both variables are related to each other [41]. For this part of the analysis, the PAleontological STatistics (PAST) program was used for identifying and investigating the lag time with the highest correlation value, for use in developing the multiple linear regression model later.

Lastly, when the proper lag time between the climate/oceanology and the rainfall is found, the multiple linear regression model – which shows the relationship between Y and $X_1, X_2, \ldots, X_m$ – is developed as follows:

$$Y_t = b_0 + b_1 X_1 + b_2 X_2 + \cdots + b_m X_m \tag{5}$$

where Y (the dependent variable) is the amount of rainfall at each t station, X_m (an independent variable) is the value from each of the six climate indices, b_0 is the Y intercept, and b_1 is the regression coefficient of the independent variable X_i when the other independent variables are fixed. Data from 1980-2010 were used for calibration, data from 2011-2014 for verification, and data from 2015 were used for forecasting. The Statistical Package for the Social Sciences (SPSS) [42] was used for this part of the analysis.

4. **Results and Discussion.**

4.1. **Climatic indices return periods.**

Based on data analysis, the climate/oceanography variability phenomenon is composed of the Asian Summer Monsoon, Indian Ocean Dipole, and El Niño-Southern Oscillation. There are six indices in total, and the resulting spectral analysis and wavelet transform are presented in Figure 5.

Figure 5(a) illustrates the periodograms of the IMI index analyzed using the PAST program, and shows that the periodicity of the strongest peak in the spectrum is 1 year. The second strongest peak is smaller and the periodicity is around 0.5 years, or 6 months.

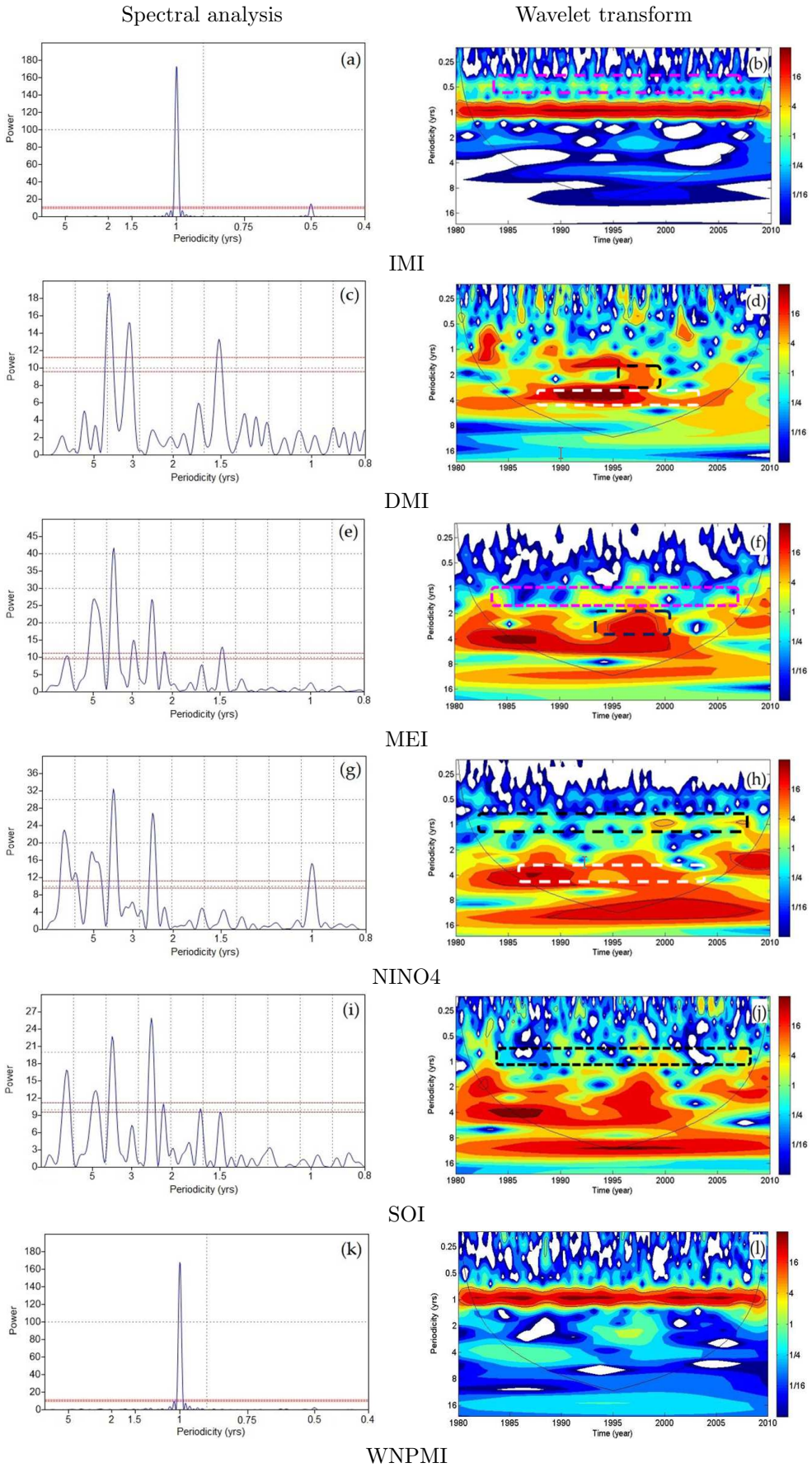

FIGURE 5. (color online) Periodograms of the climate condition index taken from the spectral analysis and the wavelet transform

The two red dashed lines are the $p < 0.01$ (upper line) and $p < 0.05$ significance levels with respect to white, uncorrelated noise.

The wavelet analysis results were presented on the x-, y- and z-axes of the contour wavelet plots, respectively representing time of measurement, periodicity, and power proportional. The relatively significant power signifies reasonably greater significance for particular frequencies in explaining the oscillation in the IMI time series, considering only the data above the Cone of Influence (COI) which is the region of the wavelet spectrum in which the edge effects become significant (defined as the e-folding time for the autocorrelation of wavelet power at each scale) [36].

Figure 5(b) shows that the highest peak was established around 1 year into the studied period. In addition, the next obvious periodicity is at around the 6 month mark, which will appear on and off throughout the studied time period (pink dashed lines). This is consistent with studies on the rainfall variability caused by the summer monsoon, which has a seasonal and annual variability period that was outlined by Hendon et al. [43], Higgins and Shi [44] and Chen et al. [45].

The DMI index monthly data was also analyzed, as shown in Figure 5(c). From the periodograms, three peaks above the significance level line can be clearly seen. The strongest peak is at about 4 years, the second strongest peak is at about 3 years, and the third strongest peak is at about 1.5 years. Figure 5(d) shows the return period from the wavelet transform. The strongest is at about four year periodicity, between approximately 1990 and 1996. Also shown is a low peak from 1986 through to 2004 (white dashed lines). However, the next strongest peak is at about 2-3 years and occurs in the period between 1996-2000 (black dashed lines). Considering Figure 5(c) together with Figure 5(d) could help improve confidence in estimating the return period. This result is in consistent with the research of Saji et al. [5] and Yamagata et al. [6], who found that the IOD phenomenon has an annual recurrence period.

Figure 5(e) shows that the MEI index has many peaks above the significance level. The highest amplitude is at around 4 years, the next strongest peak is at 5 years, and the third is at around 2.5 years. In terms of the wavelet transform, Figure 5(f) shows that the strongest peak is established at around 4 years, which is consistent with the results from the spectral analysis, and further wavelets that are strong were found in 1986 and 1988. In addition, the next strongest peaks were found to have a 2-3 year periodicity between 1994 and 2000 (black dashed lines). Spectral analysis can help identify the high peaks more conveniently. Moreover, the study result is consistent with Wigley [46] and Trenberth and Shea [47], who found that the MEI index that shows the ENSO phenomenon has variability in the inter-annual and long-term.

The NINO4 index in Figure 5(g) shows the strongest peak at around 3.8 years. At the same time, Figure 5(h) shows the strongest peak at around 4 years, between 1996-1998, and also shows a low peak from 1986 through to 2004 (white dashed lines). In addition, other small peaks, such as at 1, 2, or 3 year periodicity, appeared throughout the study period. The above fundamental step could be used to find the cyclicity of the SOI index, as shown in Figures 5(i) and 5(j). The strongest peak occurs at approximately 4 years for both the spectral analysis and wavelet transform. From the analyzed results, the MEI, NINO4, and SOI indexes all have their strongest peak at about 4 years. This is because all of the indices above are anomaly indexes of ENSO, with differences in the estimate variables and regions.

Lastly, the WNPMI index data in Figures 5(k) and 5(l) demonstrates cyclicity that can be interpreted as a significant round appearing about once per year, which is similar to the IMI index because they are both variables that explain the summer monsoon occurrence but differ in the area for estimation.

The return period analysis, using the spectral analysis and the wavelet transform, effectively identified the periodicity of the variables since the wavelet transform is quite detailed. The return period of the indices from the spectral analysis can be easily described by the characteristics throughout the data by assuming it is somewhat stationary, despite the absence of the same peak in the inter-annual and multi-decadal periods, as can be seen in Table 2.

TABLE 2. The highest amplitudes of the return period of the climate condition/oceanography index by spectral analysis

Index	**Highest Return Period (Years)**		
	First	Second	Third
IMI	1.0	0.5	–
DMI	4.2	3.0	1.5
MEI	3.9	5.2	2.4
NINO4	3.8	2.5	12.4
SOI	2.4	3.9	11.6
WNPMI	1.0	–	–

4.2. **Rainfall return periods.** Although the rainfall data from the 15 gauging stations in the study area was collected between 1951 to present time, each station has a different collecting time period. The data analyzed in the study was from 1980-2014 as this time period had a complete dataset. In the analysis of rainfall, spectral analysis and wavelet analysis were used to identify and investigate periodicities in the time series data.

Figure 6 illustrates the behavior of the recurrence periods of rainfall at three sample stations (Bangkok station, Nakhon Pathom station, and Nakhon Sawan station). To analyze the monthly rainfall, spectral analysis and the wavelet transform were applied, and the periodicity of strongest peak was found to occur at 1 year. The next lowest peak was at about 0.5 years, and another peak occurred at about 0.33 years, or 4 months. Accordingly, rainfall behavior is found in each season and the results are similar at every station that was studied.

As discussed in Section 4.1, the analysis of the recurrence period of the climate/oceanography index revealed that the recurrence periods of the Indian Summer Monsoon Index and Western North Pacific Index are similar, occurring at about 1 year, which is in accordance with the level of rainfall. This makes possible an assertion of their interrelation, and can therefore allow accurate rainfall prediction. With regards to ENSO, there are three variables of interest – namely the Multivariate ENSO Index (MEI), the South Oscillation Index (SOI), and the Sea Surface Temperature (NINO4). The major recurrence period of the MEI is about 4 years and, in addition, 1 year and 6 month periodicity were also found (Figures 5(e) and 5(f)) between 1983 and 1987 and between 1996 and 1999, which would have influenced the rainfall. For NINO4, the 1 year and 6 month periodicities are also found (Figures 5(g) and 5(h)). Figure 5(j) also shows the 1 year and 6 month periodicity. This pattern appears throughout almost the entire data set, so it is assumed to be somewhat stationary. This means that it would be possible to use such a climate index with multiple regression for forecasting rainfall. However, the results from the regression analysis between the climatic indices and rainfall at the same initial time (without lag time) did not produce good rainfall forecasts. Therefore, the cross-correlation was used to determine the appropriate lag time between the index and rainfall.

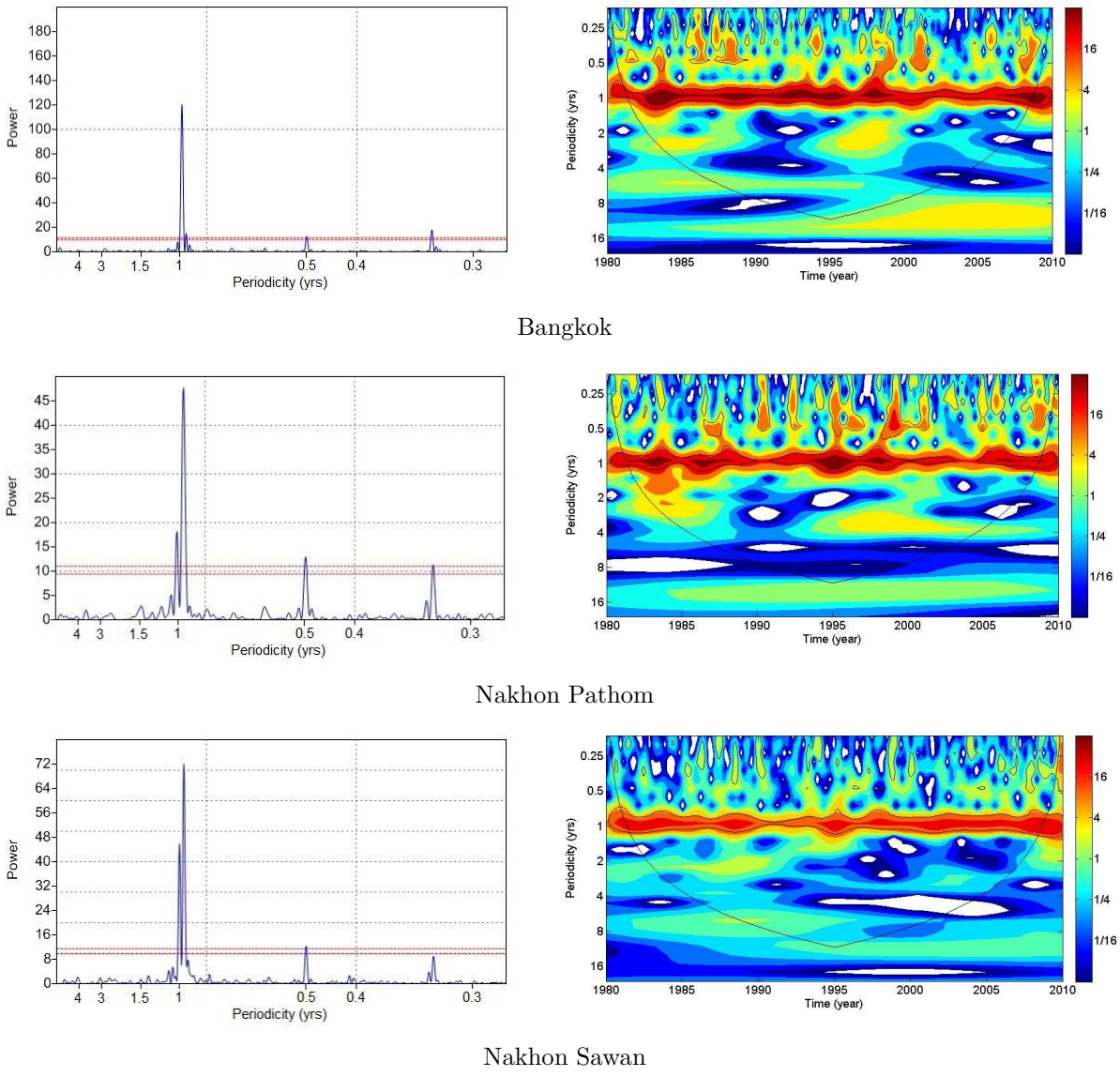

FIGURE 6. (color online) Analysis of the recurrence period of monthly rainfall for sample stations

4.3. **Linkage between climatic signals and rainfall by cross-correlation.** According to the analysis in Section 4.2, the climate/oceanography index has a cyclicity that corresponds to the rainfall. Therefore, the cross-correlation of the six indices includes IMI, WNPMI, DMI, MEI, SOI, and NINO4, which were applied along with the rainfall at the 15 stations of the study area in order to correlate (compare) two time series using a range of possible alignments, until a good match was found. The important applications in this process include the correlation and the identification of delay times between two measured parameters.

Figure 7 illustrates the relationship between the parameters throughout the study period. In the figure, the positive lag values mean that the climate index is leading while negative lags mean the rainfall is leading. We hypothesized that the actual relationship should be that the climate index is leading and correlated in the same direction with the rainfall. The climate index data was shown to have a correlation to the rainfall, and the cyclic pattern on the lag axis shown throughout is due to the periodicities in the signals. Therefore, the highest positive correlation of the first cycle from the initial point (0-lag)

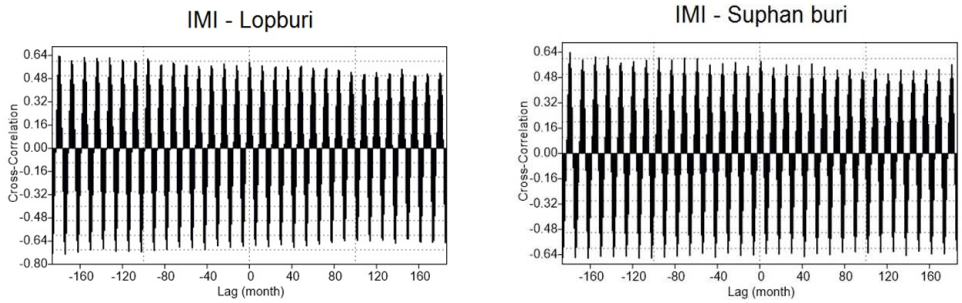

(a)

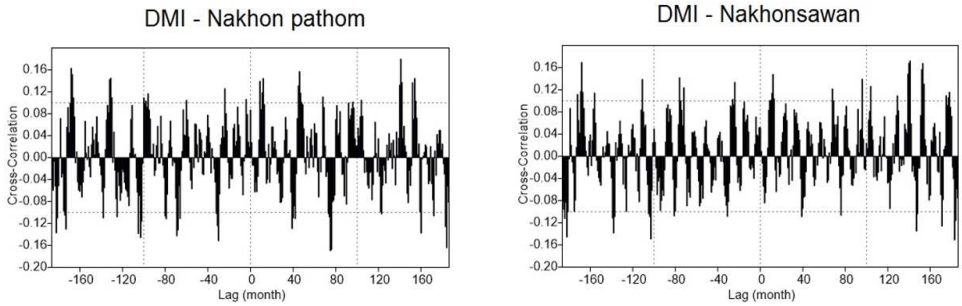

(b)

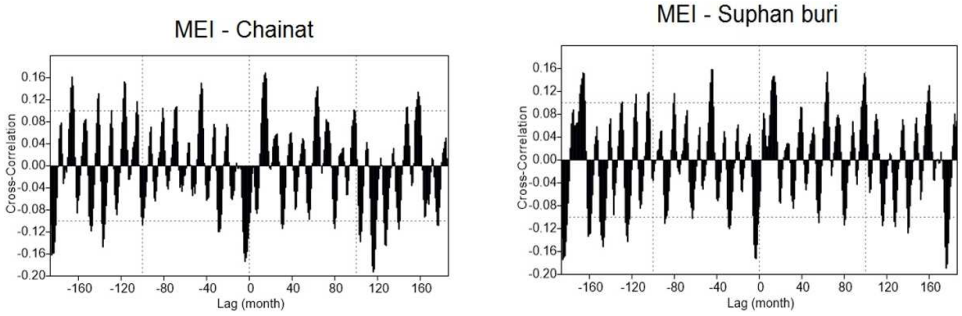

(c)

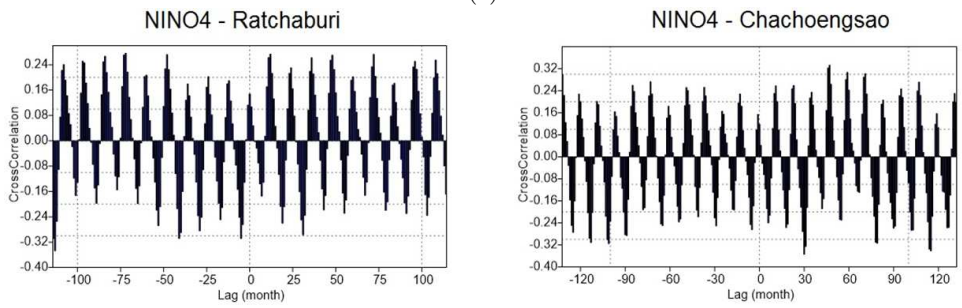

(d)

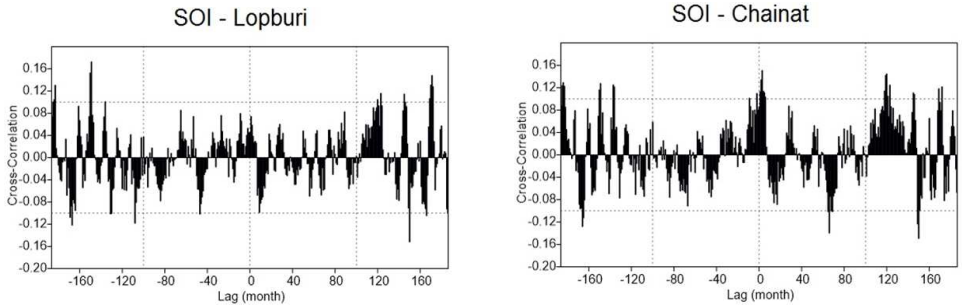

(e)

FIGURE 7. The characteristics of cross-correlation among the (a) IMI; (b) DMI; (c) MEI; (d) NINO4, and (e) SOI Index and the monthly rainfall

TABLE 3. The selected lag time between the rainfall and the studied indices from the cross-correlation

Station	Lag with Maximum Correlation (Months)					
	IMI	WNPMI	DMI	MEI	SOI	NINO4
Bangkok	12	12	12	12	1	12
Chainat	12	12	12	15	3	12
Lopburi	12	12	9	13	1	11
Suphan Buri	11	12	12	14	2	12
Nakhon Pathom	12	12	12	13	2	12
Ayutthaya	12	12	11	13	6	11
Nakhon Sawan	12	12	12	12	1	11
Pathum Thani	12	12	12	13	6	11
Kanchanaburi	11	12	9	14	2	12
Chachoengsao	12	12	8	7	6	11
Ratchaburi	11	12	12	12	5	12
U-Thong	11	12	9	13	2	12
Takfa	12	12	11	13	3	12
Kamphaeng Phet	12	12	13	14	2	12
Don Mueang	12	12	9	13	2	12

and the time delay is considered suitable to use for the regression analysis. The selected lag times between the rainfall and the studied indices from the cross-correlation are shown in Table 3. In addition, if the time that gave the highest correlation throughout the whole dataset was considered, there would be less data for the regression analysis.

Each climate index shows a different highest associated result. IMI has a medium to high correlation value, overall scoring between 0.5 and 0.7. The highest correlation value (0.67) was found at Nakhon Sawan station, whereas the lowest value (0.482) was found at Kanchanaburi station. According to the lag time graph shown in Figure 7(a), the rainfall rapidly responded to the IMI index. This is consistent with previous studies claiming that IMI is a measure of the summer monsoon. The highest correlation coefficient value for cyclicity throughout the lag axis was found to be similar at every rain gauge station. However, the lag time that is shown in Table 3 is from the next positive peak correlation from the lag-zero, to suit the predictive equations.

The association between DMI and the monthly rainfall of individual stations presents with a low correlation coefficient value, as was the case for the station in Figure 7(b). In general, the value is between 0.1-0.2. The highest and lowest correlation values were found at Pathum Thani station (0.180) and Lop Buri station (0.008), respectively. Based on the lag time shown in Table 3, it was found that every rainfall was highly associated with DMI with a time delay about 9-12 months.

Regarding MEI, there was a low correlation value, similar to that found in DMI, which was generally between 0.1-0.2. The highest correlation value (0.180) was found at Kamphaeng Phet station, while the lowest correlation value was 0.083. Based on Figure 7(c), for the Chainat and Ratchaburi stations, it was found to be at about 15 and 12 months, respectively. The lag time in Table 3 shows that rainfall is highly associated with MEI in 7-15 month intervals.

Regarding the association between the climate index (NINO4) and the monthly rainfall of every station in the study area, the correlation coefficient value during the studied period was medium overall (0.2-0.7). The highest correlation value (0.65) was found at Takfa station, Nakhon Sawan province; meanwhile, the lowest correlation value was 0.22,

found at Kanchanaburi station. Figure 7(d) shows the rainfall associated with the NINO4 index of the Chachoengsao and Ratchaburi station at 11 and 12 months, respectively. Table 3 shows that the time lag of every station is about 11-12 months.

In general, SOI has low correlation value between 0.1-0.2. The highest and lowest correlation values were found at Pathum Thani station (0.19) and Thakfa station (0.07), respectively. Based on the lag time graph in Figure 7(e), it was found that the amount of rainfall is highly associated with SOI in Lopburi and Chainat at lag time about 1 and 3 months, respectively.

For the WNPMI index the figure is not displayed because it resembled the IMI index; however, it was found to have a medium to high correlation value, in general scoring between 0.5-0.7. The highest correlation value (0.66) was found at Nakhon Sawan station, while the lowest (0.51) was found at Pathum Thani station. Table 3 presents the lag times that are associated with the rainfall, as well as each climate condition/oceanography index. These lag times of the climate index were used in accordance with the multiple regression equation to obtain an equation composed of independent and dependent variables that had the most suitable linear relationship without lag time multiple regression.

In conclusion, the lag times of the WNPMI, IMI, and NINO4 to the rainfall, found by the cross-correlation, were very evident – especially at the peak of lag-0. Since the data exhibited a cyclic pattern, regression analysis with the lag time of the independent variables can be applied. This set of index lag times was identified as the lag times with the next positive peak correlations from lag-0, to suit the predictive equations.

4.4. **Multiple regression analysis.** From the analysis in the previous sections, the spectral analysis and wavelet transform indicate an association between climate condition/oceanography and the rainfall, and the most suitable lag time with strongly associated variables was discovered using cross-correlation. Consequently, a multiple regression equation was used to obtain an independent and dependent variable equation with a linear relationship. In this study, the independent variable was the climate/oceanography index, while the dependent variable was rainfall. The multiple linear regression analysis could be divided into two cases; the model with lag time and the model without lag time. The SPSS program was applied during independent variable selection using the stepwise equation method. Stepwise linear regression is a method of regressing multiple variables while simultaneously removing those that are not important.

Figure 8 presents an example of the stepwise regression with lag time for rainfall data at the Bangkok station, which was analyzed by the program. Consequently, the results show that WNPMI was associated with the dependent variable. DMI and SOI are significantly correlated with rainfall; therefore, this was further analyzed in the equation. Other independent variables that did not have a significant relationship with rainfall were deleted.

The association between the average monthly rainfall and the climate condition/oceanography index was analyzed to find the result of the multiple regression equation at each station. The results of the lag time regression are better than those without lag time regression; therefore, Table 4 shows only those results with lag time regression included. It was found that the minimum value of the multiple coefficient correlation (R), 0.570, was scored at U-thong station, while the maximum value, 0.703, was derived at Nakhon Sawan station. In addition, WNPMI is the most influential of the indices on monthly rainfall in the all regression equations. The next most influential are SOI, MEI, and DMI, respectively. In comparison with the other indices, WNPMI is the variable that is most associated with rainfall in the studied areas, conforming to the analysis of the cross-correlation in the previous section.

Model Summary

Model	R	R Square	Adjusted R Square	Std. Error of the Estimate
1	.631[a]	.398	.397	105.62370
2	.645[b]	.416	.413	104.20322
3	.653[c]	.426	.421	103.46445

a. Predictors: (Constant), wnpmi

b. Predictors: (Constant), wnpmi, dmi

c. Predictors: (Constant), wnpmi, dmi, soi

Coefficients[a]

Model		Unstandardized Coefficients		Standardized Coefficients	t	Sig.
		B	Std. Error	Beta		
1	(Constant)	164.166	5.615		29.238	.000
	wnpmi	14.263	.897	.631	15.907	.000
2	(Constant)	152.279	6.556		23.226	.000
	wnpmi	14.090	.886	.624	15.902	.000
	dmi	57.036	16.830	.133	3.389	.001
3	(Constant)	153.555	6.529		23.518	.000
	wnpmi	14.212	.881	.629	16.130	.000
	dmi	49.491	16.972	.115	2.916	.004
	soi	13.590	5.347	.100	2.542	.011

a. Dependent Variable: rain Bangkok

FIGURE 8. Example of an analysis of climate index and rainfall at the Bangkok station by means of stepwise analysis with the lag time

Validation of the equations in Table 4 was carried out by using data for the rainfall at each station for the years 2011-2014. It was found that the equations represent the amount of rain that fell reasonably well, as shown in Figure 9 and in the comparison of the statistical data and rainfall in Table 5. It was found that the means are similar for both the observed data and the validated data. The notification information has the characteristic of skewing to the right. In the case of kurtosis, most of the observed data have a positive trend, but for the validated data, the kurtosis is negative. Consequently, the prediction model tends to underestimate extreme precipitation, which is one aspect that needs to be improved.

Figure 10 illustrates forecasting for the year 2015. The scatter plot shows the comparison of rainfall prediction from the regression equation in Table 4 with the rainfall obtained from the observed data. These were presented in order to figure out the coefficient of determination value (R^2). Overall, of the 15 rainfall gauging stations, the highest coefficient determination value (0.73) was found at Kamphaeng Phet station. On the other hand, the lowest coefficient determination value (0.34) was found at Chainat station.

In general, the derived regression model can explain the variance of the rainfall spread around the average quite well. Although the correlations of DMI, SOI, NINO4, and MEI with the rainfall are minimal, these factors affected the regression equation analysis in general and increased the value of the regression coefficient (R) derived at some stations.

In addition, the regression model was used for confirmation of accuracy by using the Relative Root Mean Square Error (RRMSE) index. If the RRMSE value was greater than

TABLE 4. Multiple regression with the lag time equation and multiple coefficient correlation (R) between rainfall and the climate condition/oceanography indices

Station	Equation	R	Most Effective
Bangkok	$Y_t = 153.55 + 14.21WNPMI_{t-12} + 49.49DMI_{t-12} + 13.590SOI_{t-1}$	0.653	DMI
Chainat	$Y_t = 95.47 + 7.29WNPMI_{t-12} + 14.47MEI_{t-15} + 12.1SOI_{t-3} + 2.67IMI_{t-12}$	0.648	MEI
Lopburi	$Y_t = 111.55 + 10.07WNPMI_{t-12} + 8.60SOI_{t-1}$	0.645	WNPMI
Suphan Buri	$Y_t = 93.43 + 9.08WNPMI_{t-12} + 11.81MEI_{t-14} + 10.72SOI_{t-2}$	0.623	MEI
Nakhon Pathom	$Y_t = 100.30 + 9.28WNPMI_{t-12} + 11.75SOI_{t-2}$	0.617	SOI
Ayutthaya	$Y_t = 99.67 + 7.62WNPMI_{t-12} + 2.76IMI_{t-12} + 17.64MEI_{t-13} + 16.1SOI_{t-6}$	0.685	MEI
Nakhon Sawan	$Y_t = 111.79 + 7.53WNPMI_{t-12} + 3.83IMI_{t-12} + 13.1SOI_{t-1}$	0.703	SOI
Pathum Thani	$Y_t = 130.03 + 10.89WMPMI_{t-12} + 15.7SOI_{t-6}$	0.618	SOI
Kanchanaburi	$Y_t = 98.05 + 8.40WMPMI_{t-12} + 12.92MEI_{t-14} + 11.67SOI_{t-2}$	0.574	MEI
Chachoengsao	$Y_t = 126.73 + 6.79WNPMI_{t-12} + 4.01IMI_{t-12} + 9.69SOI_{t-6}$	0.649	SOI
Ratchaburi	$Y_t = 116.12 + 10.9WNPMI_{t-12}$	0.641	WNPMI
U-Thong	$Y_t = 91.48 + 8.4WNPMI_{t-12} + 10.25SOI_{t-2} + 30.0DMI_{t-9}$	0.570	SOI
Takfa	$Y_t = 111.69 + 7.19WNPMI_{t-12} + 4.18IMI_{t-12} + 11.48MEI_{t-13}$	0.673	MEI
Kamphaeng Phet	$Y_t = 120.16 + 8.07WNPMI_{t-12} + 4.39IMI_{t-12} + 11.66SOI_{t-2} + 35.0DMI_{t-13}$	0.682	DMI
Don Mueang	$Y_t = 130.13 + 7.63WNPMI_{t-12} + 16.37SOI_{t-2} + 4.37IMI_{t-12}$	0.646	SOI

1, it meant that the regression model with lag time forecasting had less error than the regression model without lag time forecasting. Table 6 shows the comparison and RRMSE values between the regression with the lag time model and the regression without the lag time model. At all stations, the forecast results of the regression with the lag time model had obviously fewer errors than the regression without the lag time model. This means that including lag time in the model results in more accurate forecasting.

5. **Conclusions.** This study assesses the impact of climate oscillation/oceanography stemming from the Indian Ocean Dipole (IOD), El Niño-Southern Oscillation (ENSO), and Asian Summer Monsoon (ASM). Spectral analysis and wavelet analysis were used to identify and investigate periodicities in a time series. The wavelet transformation explains the return period of each set of time series data effectively, especially when there are the non-stationary data in the set [32,48]. At the same time, since there are some short return period values presented, spectral analysis was also used to show the highest return period for a stationary time series.

Overall, the recurrence period of DMI is about 1.5-4 years, while the recurrence period of MEI is about 2.5-5 years. The recurrence period of SOI is 2.5-4 years and 12 years.

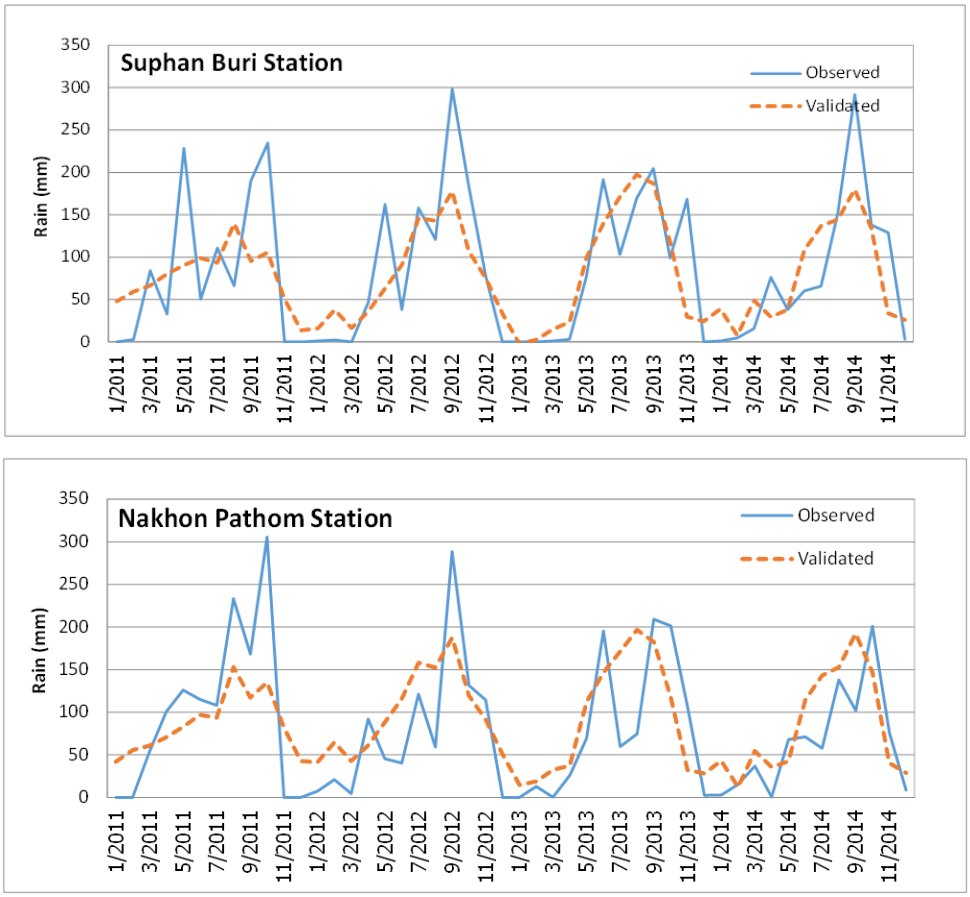

FIGURE 9. Examples of rainfall verification and the actual rainfall time series, derived from the studied areas in 2011-2014

TABLE 5. Descriptive statistics of the rainfall data for the lag time model validation periods for 2011-2014

Station	Observed Data			Validated Data		
	Mean	Skewness	Kurtosis	Mean	Skewness	Kurtosis
Bangkok	140.12	0.933	0.161	150.651	0.592	−0.838
Chainat	92.50	1.165	1.291	84.535	0.328	−1.293
Lopburi	87.48	1.093	0.654	97.416	0.474	−1.161
Suphan Buri	85.00	0.794	0.240	79.445	0.453	−0.928
Nakhon Pathom	80.63	1.075	0.631	89.647	0.426	−1.072
Ayutthaya	90.22	0.921	−0.043	91.617	0.243	−1.300
Nakhon Sawan	94.45	0.840	0.108	90.353	0.346	−1.249
Pathum Thani	104.14	1.200	0.768	122.010	0.384	−1.303
Kanchanaburi	82.73	0.787	0.156	85.498	0.422	−0.898
Chachoengsao	139.43	1.126	1.492	119.991	0.373	−1.491
Ratchaburi	87.63	0.679	−0.553	96.402	0.523	−1.160

Lastly, the recurrence period of Sea Surface Temperature (NINO4) is also 2.5-4 years and 12 years, consistent with the El Nino phenomenon [49,50]. The above data show the characteristics of interannual and interdecadal scales. According to this study of rainfall data analysis derived from 15 gauging stations in the central plain of Thailand, it was

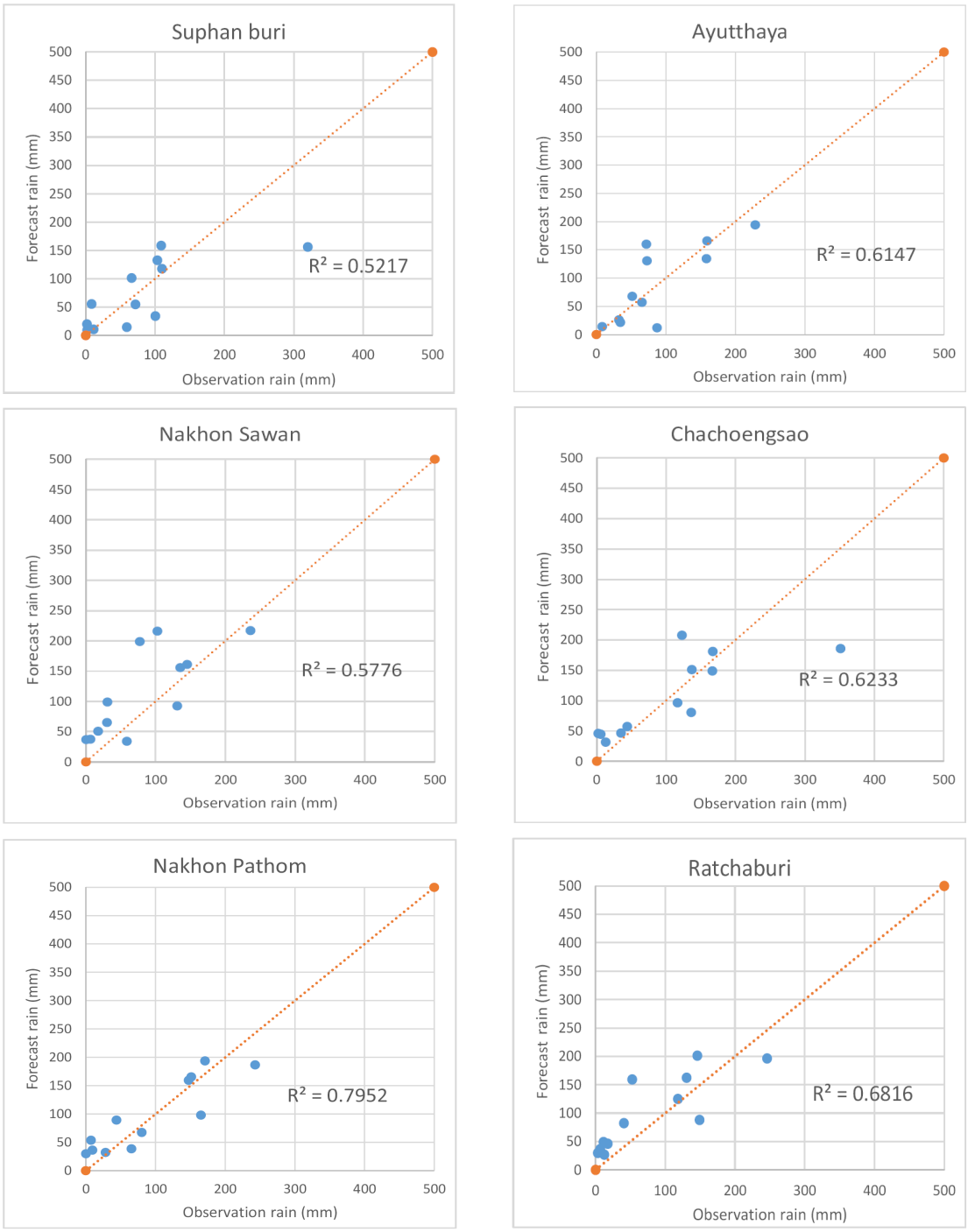

FIGURE 10. Comparison of predicted rainfall with observed rainfall and the value of R^2, in the year 2015

found that monthly rainfall data provides the most obvious 1 year recurrence period, and this finding was consistent at every station. In addition, the results coincided with the rainy season in Thailand.

Based on the analysis of cross-correlation between the variables IMI, WNPMI, DMI, MEI, SOI, and NINO4 and the rainfall derived from stations in central plain of Thailand, the correlation coefficient value of DMI and MEI with rain is minimal (0.1-0.2). Regarding the cross-correlation between the IMI and WNPMI, it was found that these indices are

TABLE 6. Comparison of accuracy of forecasting with the lag time model and without the lag time model

Station	(1) RMSE (Without lag)	(2) RMSE (With lag)	(3) = (1)/(2) RRMSE
Bangkok	109.72	110.79	0.990
Chainat	55.56	57.34	0.969
Lopburi	69.58	60.86	1.143
Suphan Buri	59.99	58.35	1.028
Nakhon Pathom	37.65	35.97	1.047
Ayutthaya	54.32	43.37	1.252
Nakhon Sawan	59.50	57.74	1.031
Pathum Thani	57.98	51.26	1.131
Kanchanaburi	69.95	66.93	1.045
Chachoengsao	59.93	59.81	1.002
Ratchaburi	44.26	47.87	0.925
U-Thong	67.16	65.44	1.026
Takfa	55.13	54.96	1.003
Kamphaeng Phet	52.20	42.57	1.226
Don Mueang	87.33	78.45	1.113

highly associated with monthly rainfall; the associations are greater than those of the other indices, and the coefficient correlation value is approximately 0.6. It was noticed that the summer monsoon plays an important role in rainfall over a very short period of time, or is effective immediately (peak on 0-lag), since analysis of SOI showed an impact on rainfall when it was over a 1 month period.

Moreover, based on the analysis of the multiple regression equation between the climate condition index and rainfall, the regression with lag time forecast better than that without lag time, with this result being supported by the RRMSE index. WNPMI is the most significant index for its influence on rainfall at the stations in the study area. The next most influential climates are SOI, MEI, and DMI, respectively. In general, the multiple correlation coefficient values (R) of all stations are between 0.570-0.703. According to the investigation of multiple equation prediction and rainfall data in 2015, the forecast is accurate. The highest value of R^2, derived at Kampang Phet station, was 0.73.

This study demonstrated that applying statistical analysis to the study and assessment of the relationship between the climate and the rainfall could be very useful for planning water use for sustainable development. It is clear that the response of rainfall to climatic factors is delayed. In the future, examination of indices involving other climate factors will be undertaken. Many sectors have been studied in this manner and these results could lead to better rainfall prediction. In the past few decades many more modeling techniques have been proposed for research in hydrological modeling, such as Artificial Neural Networks (ANNs). It may be useful if these techniques are also applied to precipitation analysis.

Acknowledgment. For the successful research completion, the corresponding author would like to extend his deep gratitude to the Bureau of Meteorology and KMITL for the data they provided. The authors would like to acknowledge the support and cooperation of these institutions. The authors are also sincerely grateful to the anonymous reviewers for providing thorough reviews and useful suggestions.

REFERENCES

[1] T. R. Green, M. Taniguchi, H. Kooi, J. J. Gurdak, D. M. Allen, K. M. Hiscock et al., Beneath the surface of global change: Impacts of climate change on groundwater, *Journal of Hydrology*, vol.405, pp.532-560, 2011.

[2] R. Hanson, M. Newhouse and M. Dettinger, A methodology to asess relations between climatic variability and variations in hydrologic time series in the southwestern United States, *Journal of Hydrology*, vol.287, pp.252-269, 2004.

[3] J. L. McBride and N. Nicholls, Seasonal relationships between Australian rainfall and the southern oscillation, *Monthly Weather Review*, vol.111, pp.1998-2004, 1983.

[4] D. L. Hartmann, A. M. G. K. Tank, M. Rusticucci et al., *Climate Change 2013: The Physical Science Basis, Contribution of Working Group I to the Fifth Assessment Report of the Intergovernmental Panel on Climate Change*, Cambridge University Press, Cambridge, 2013.

[5] N. Saji, B. Goswami, P. Vinayachandran and T. Yamagata, A dipole mode in the tropical Indian Ocean, *Nature*, vol.401, p.360, 1999.

[6] T. Yamagata, S. K. Behera, J. J. Luo, S. Masson, M. R. Jury and S. A. Rao, Coupled ocean-atmosphere variability in the tropical Indian Ocean, *Earth's Climate*, pp.189-211, 2004.

[7] G. Gu, R. F. Adler, G. J. Huffman and S. Curtis, Tropical rainfall variability on interannual-to-interdecadal and longer time scales derived from the GPCP monthly product, *Journal of Climate*, vol.20, pp.4033-4046, 2007.

[8] B. M. Buckley, K. Palakit, K. Duangsathaporn, P. Sanguantham and P. Prasomsin, Decadal scale droughts over northwestern Thailand over the past 448 years: Links to the tropical Pacific and Indian Ocean sectors, *Climate Dynamics*, vol.29, pp.63-71, 2007.

[9] Ö. Terzi and E. Çevik, Rainfall estimation using artificial neural network method, *SDU International Journal of Technological Science*, vol.4, 2012.

[10] T. Tingsanchali and M. R. Gautam, Application of tank, NAM, ARMA and neural network models to flood forecasting, *Hydrological Processes*, vol.14, pp.2473-2487, 2000.

[11] N. Singhrattna, B. Rajagopalan, M. Clark and K. K. Kumar, Seasonal forecasting of Thailand summer monsoon rainfall, *International Journal of Climatology*, vol.25, pp.649-664, 2005.

[12] T. Murakami and J. Matsumoto, Summer monsoon over the Asian continent and western North Pacific, *Journal of the Meteorological Society of Japan. Ser. II*, vol.72, pp.719-745, 1994.

[13] J. J. Gurdak, R. T. Hanson, P. B. McMahon, B. W. Bruce, J. E. McCray, G. D. Thyne et al., Climate variability controls on unsaturated water and chemical movement, High Plains Aquifer, USA, *Vadose Zone Journal*, vol.6, pp.533-547, 2007.

[14] S. Philander, *El Nifio, La Nifia, and the Southern Oscillation*, Academic Press, 1990.

[15] N. J. Mantua and S. R. Hare, The Pacific decadal oscillation, *Journal of Oceanography*, vol.58, pp.35-44, 2002.

[16] S. Minobe, A 50-70 year climatic oscillation over the North Pacific and North America, *Geophysical Research Letters*, vol.24, pp.683-686, 1997.

[17] F. K. Fye, D. W. Stahle, E. R. Cook and M. K. Cleaveland, NAO influence on sub-decadal moisture variability over central North America, *Geophysical Research Letters*, vol.33, 2006.

[18] R. A. Kerr, A North Atlantic climate pacemaker for the centuries, *Science*, vol.288, pp.1984-1985, 2000.

[19] F. H. Chiew, T. C. Piechota, J. A. Dracup and T. A. McMahon, El Nino/Southern Oscillation and Australian rainfall, streamflow and drought: Links and potential for forecasting, *Journal of Hydrology*, vol.204, pp.138-149, 1998.

[20] K. Wolter and M. S. Timlin, Monitoring ENSO in COADS with a seasonally adjusted principal component index, *Proc. of the 17th Climate Diagnostics Workshop*, 1993.

[21] D. R. Cayan, El Niño/southern oscillation and streamflow in the western United States, *El Niño, Historical and Paleoclimatic Aspects of the Southern Oscillation*, pp.29-68, 1992.

[22] A. Limsakul, S. Limjirakan and B. Suthamanuswong, Spatiotemporal changes in total annual rainfall and the annual number of rainy days in Thailand, *Journal of Environmental Research*, vol.29, pp.1-21, 2007.

[23] K. Kusreesakul, *Spatio-Temporal Rainfall Changes in Thailand and Their Connection with Regional and Global Climate Variability*, Master Thesis, Prince of Songkla University, 2009.

[24] A. Limsakul and J. I. Goes, Empirical evidence for interannual and longer period variability in Thailand surface air temperatures, *Atmospheric Research*, vol.87, pp.89-102, 2008.

[25] A. Limsakul, S. Limjirakan and B. Suttamanuswong, Asian summer monsoon and its associated rainfall variability in Thailand, *Environment Asia*, vol.3, pp.79-89, 2010.
[26] N. Satellite, *Information Service*, National Climatic Data Center, US Department of Commerce, 2012.
[27] A. Papoulis, *The Fourier Integral and Its Applications*, 1962.
[28] R. B. Blackman and J. W. Tukey, The measurement of power spectra from the point of view of communications engineering – Part I, *Bell Labs Technical Journal*, vol.37, pp.185-282, 1958.
[29] Ø. Hammer and D. Harper, Chapter 4 Morphometrics, in *Paleontological Data Analysis*, Blackwell Publishing, Malden, Oxford & Carlton, 2006.
[30] Ø. Hammer, PAST: Paleontological statistics software package for education and data analysis, *Palaeontologia Electronica*, vol.4, p.9, 2001.
[31] D. Harper, *Numerical Palaeobiology: Computer-based Modelling and Analysis of Fossils and their Distributions*, Media CD, Version: 1.11, John Wiley & Sons, 1999.
[32] M. Misiti, Y. Misiti, G. Oppenheim and J. Poggi, *Wavelet Toolbox 4 User's Guide*, The MathWorks, Natick, MA, 2007.
[33] U. Seeboonruang, Wavelet relationship between climate variability and deep groundwater fluctuation in Thailand's Central Plains, *KSCE Journal of Civil Engineering*, vol.22, pp.868-876, 2018.
[34] J. J. Gurdak, R. T. Hanson, P. B. McMahon, B. W. Bruce, J. E. McCray, G. D. Thyne et al., Climate variability controls on unsaturated water and chemical movement, High Plains aquifer, USA, *Vadose Zone Journal*, vol.6, pp.533-547, 2007.
[35] K. Lau and H. Weng, Climate signal detection using wavelet transform: How to make a time series sing, *Bulletin of the American Meteorological Society*, vol.76, pp.2391-2402, 1995.
[36] C. Torrence and G. P. Compo, A practical guide to wavelet analysis, *Bulletin of the American Meteorological Society*, vol.79, pp.61-78, 1998.
[37] I. De Moortel, S. Munday and A. Hood, Wavelet analysis: The effect of varying basic wavelet parameters, *Solar Physics*, vol.222, pp.203-228, 2004.
[38] C. Moler, *MATLAB Users' Guide*, University of New Mexico, 1982.
[39] M. Rutulis, Groundwater drought sensitivity of southern Manitoba, *Canadian Water Resources Journal*, vol.14, pp.18-33, 1989.
[40] P. Bourke, *Cross Correlation, Auto Correlation, 2D Pattern Identification*, 1996.
[41] J. Higgins, Introduction to multiple regression, *The Radical Statistician*, vol.1, pp.1-15, 2005.
[42] N. H. Nie, D. H. Bent and C. H. Hull, *SPSS: Statistical Package for the Social Sciences*, McGraw-Hill, New York, 1970.
[43] H. H. Hendon, C. Zhang and J. D. Glick, Interannual variation of the Madden-Julian oscillation during austral summer, *Journal of Climate*, vol.12, pp.2538-2550, 1999.
[44] R. Higgins and W. Shi, Intercomparison of the principal modes of interannual and intraseasonal variability of the North American monsoon system, *Journal of Climate*, vol.14, pp.403-417, 2001.
[45] T.-C. Chen, M.-C. Yen and S.-P. Weng, Interaction between the summer monsoons in East Asia and the South China Sea: Intraseasonal monsoon modes, *Journal of the Atmospheric Sciences*, vol.57, pp.1373-1392, 2000.
[46] T. Wigley, ENSO, volcanoes and record-breaking temperatures, *Geophysical Research Letters*, vol.27, pp.4101-4104, 2000.
[47] K. E. Trenberth and D. J. Shea, Relationships between precipitation and surface temperature, *Geophysical Research Letters*, vol.32, 2005.
[48] B. Wang and Y. Wang, Temporal structure of the southern oscillation as revealed by waveform and wavelet analysis, *Journal of Climate*, vol.9, pp.1586-1598, 1996.
[49] B. Wang and Z. Fan, Choice of South Asian summer monsoon indices, *Bulletin of the American Meteorological Society*, vol.80, pp.629-638, 1999.
[50] W. S. Kessler, Is ENSO a cycle or a series of events?, *Geophysical Research Letters*, vol.29, 2002.